Biochimica et Biophysica Acta 1838 (2014) 2947–2953

Contents lists available at ScienceDirect

Biochimica et Biophysica Acta

journal homepage: www.elsevier.com/locate/bbamem

Effect of cholesterol and ergosterol on the antibiotic amphotericin B interactions with dipalmitoylphosphatidylcholine monolayers: X-ray reflectivity study

Daniel M. Kamiński [a,*], Grzegorz Czernel [b], Bridget Murphy [c,d], Benjamin Runge [c,d], Olaf M. Magnussen [c,d], Mariusz Gagoś [e,**]

[a] Department of Chemistry, University of Life Sciences in Lublin, Akademicka 15, 20-950 Lublin, Poland
[b] Department of Biophysics, University of Life Sciences in Lublin, Akademicka 13, 20-950 Lublin, Poland
[c] Institute for Experimental and Applied Physics, University of Kiel, 24098 Kiel, Germany
[d] Ruprecht Haensel Laboratory, University of Kiel, 24098 Kiel, Germany
[e] Department of Cell Biology, Institute of Biology and Biotechnology, Maria Curie-Skłodowska University, 20-033 Lublin, Poland

ARTICLE INFO

Article history:
Received 16 June 2014
Received in revised form 16 July 2014
Accepted 4 August 2014
Available online 12 August 2014

Keywords:
Amphotericin B
Lipid monolayer
Sterol
X-ray diffraction

ABSTRACT

Amphotericin B is a *Streptomyces nodosus* metabolite and one of the oldest polyene antibiotics used in the treatment of invasive systemic fungal infections. Despite its over 50-year existence in clinical practice and the recognition of amphotericin B as the gold standard in the treatment of serious systemic mycosis, it still remains one of the most toxic pharmaceuticals. Understanding of the processes at the molecular levels and the interactions between amphotericin B with lipid membranes containing sterols should elucidate the mechanisms of the action and toxicity of this widely used antibiotic. In this work, we use X-ray reflectivity to study the structural changes on a molecular scale after amphotericin B incorporation. These changes are accompanied by an increase in monolayer surface pressure which is more pronounced for ergosterol — rather than cholesterol-rich membranes. The data indicate that this difference is not due to the higher affinity of amphotericin B towards ergosterol-containing membranes but is rather due to a ~3 Angstrom corrugation of the monolayer. Furthermore, the total quantity of amphotericin B incorporated into lipid monolayers containing cholesterol and ergosterol is the same.

1. Introduction

Amphotericin B (AmB) is one of the most important drugs in the medical treatment of internal fungal infections [1,2]. The antifungal properties of AmB are related to its relatively strong interaction with ergosterol, which is the main sterol of fungal membrane, rather than with cholesterol, which occurs in mammalian cells [3–6]. Although AmB has been used clinically for a long time, its molecular organization in both biological and artificial systems as well as its mechanism of action are still of great scientific importance [3,7–15]. In this work, we discuss the effect of sterols on amphotericin B incorporation into phospholipid (DPPC) monolayers.

Surface pressure changes in monolayers in Langmuir isotherms are usually proportional to the quantity of the substances incorporated [16–19]. This simplification can be applied to many systems; however, as we show here, this is not true for AmB incorporation into lipid monolayers containing cholesterol or ergosterol. It can be found that AmB adsorbs into the DPPC–ergosterol monolayer more strongly than into the one containing cholesterol [11,16,20–22]. Using X-ray reflectivity (XRR), we show that the amount of AmB incorporated into DPPC–ergosterol and DPPC–cholesterol monolayers is the same. To explain this phenomenon and at the same time the differences in surface pressure for both systems, we propose an extension to the generally accepted superlattice model of the lipid–cholesterol monolayer [22–24]. The superlattice surface can differ not only in the in-plane arrangement of molecules but also in the out-of-plane corrugation, as found for simple binary systems [25]. In the case of such a corrugation for DPPC–cholesterol, one would expect an increase in monolayer thickness and roughness manifested by a broadening of the X-ray scattering length density (SLD) profile [26,27]. The X-ray SLD profiles determined from X-ray reflectivity data also provide information about AmB orientation and AmB mycosamine group location in the monolayer.

* Correspondence to: D.M. Kamiński, Department of Chemistry, University of Life Sciences in Lublin, 20-950 Lublin, Poland. Tel.: +48 81 4456508; fax: +48 81 4456684.
** Correspondence to: M. Gagoś, Department of Cell Biology, Institute of Biology, Maria Curie-Skłodowska University, 20-033 Lublin, Poland.
E-mail addresses: daniel_kaminski3@wp.pl (D.M. Kamiński), mariusz.gagos@poczta.umcs.lublin.pl (M. Gagoś).

http://dx.doi.org/10.1016/j.bbamem.2014.08.004
0005-2736/

2. Material and methods

The investigated monolayers were prepared from dipalmitoylphosphatidylcholine (DPPC) with purity >99%, purchased from Avanti Polar Lipids Inc.; ergosterol (>95%), amphotericin B (~95%), cholesterol (99%) and all solvents used were purchased from Sigma-Aldrich. The N-iodoacetylamphotericin B (AmB-I) was synthesized in our group, see Fig. 1. The details of the synthesis and purification are described in reference [28]. The iodoacetate group is bonded to the AmB molecule via an amine group as indicated in Fig. 1. The monolayers were prepared by slow deposition from a Hamilton glass syringe (100 μl) onto an ultrapure water surface (18.2 MΩ · cm). The chlorophorm solutions of DPPC, cholesterol, and ergosterol used had concentrations of 6.8×10^{-5} mol/dm^3. The deposited mixtures of DPPC with sterols were in a molar ratio of 1:1. The experiments were conducted in an air-conditioned hutch at 23 °C. In this study, two methods of AmB/AmB-I preparation were used. In the first method, AmB/AmB-I was dissolved in DMSO. In the second approach, fresh AmB was dissolved before every experiment in ultrapure water containing KOH to obtain a pH of 12, where AmB solubility in an aqueous solution is the highest [29,30]. Then a volume of 40 μl was injected under the monolayer into the experimental cell with an 85-ml volume. After each injection under the monolayer, the system was stabilized for 30 min by stirring (with a small magnet on the bottom of the cell cavity). The final pH was 7.2 and the AmB concentration in both methods was 2 μmol/l in the cell volume. Both preparation methods of AmB give essentially the same results.

The surface pressure and isotherms were measured with the KSV Helsinki Mini Langmuir trough purged with N_2 (relative humidity 80%) under a laminar hood.

2.1. Cell and surface diffraction

The experimental Teflon cell for X-ray reflectivity was covered with Mylar window foil. The meniscus varied between 0.3 and 0.5 mm over the cell edge. The system was continuously purged with water-saturated nitrogen (with 99.996% purity). The experiments were performed using the liquid interfaces scattering apparatus (LISA) diffractometer [31,32] at the high-resolution diffraction beamline P08 [33] of the PETRA III synchrotron at DESY at an X-ray energy of 25.05 keV. A linear Mythen detector (Dectris) was used, comprising 1280 independent detector pixels, each 50 μm high. The incoming beam was 1 mm wide and 0.1 mm high. XRR measures the intensity fraction $R(q_z)$ reflected from the interface at incidence and reflection angles α and $\beta = \alpha$, respectively, where $q_z = (4\pi/\lambda)\sin\alpha$. Due to diffuse scattering and other contributions, the background was measured by offsetting the detector by 0.5° out of the plane of reflection and subtracted from the specular signal. The scattered intensities were measured up to $q = 1.2$ Å^{-1}; however, at q above 1.0 Å^{-1} most data were at the level of the background. In all cases, data were collected over 10 orders of magnitude.

2.2. Data analysis

For the data at q lower than 0.02°, the statistical errors were increased ten times to limit their weight in the data fitting procedure. Then the model was fitted to the error weighted experimental data by the χ^2 method in the Motofit program [34] by the Abeles matrix method [35]. For the data measured in this study, the X-ray absorption by the Langmuir layers may be neglected. Because of the small number of observed fringes and weakly scattered molecules, a simple model with two layers was used for the lipid monolayers and one layer model for the pure AmB monolayer. The following parameters were employed in the fitting procedure: layer thickness, X-ray SLD for both hydrophobic (I) and hydrophilic (II) layers and the roughness at the air — layer I, layer I–layer II and layer II — solution interfaces. The scale factor was similar in all cases and in the final fitting stage was set to a constant value of 0.95 (average from all measurements). The X-ray SLD scale is defined as in Motofit, which for water is 9.43×10^{-6} A^{-2}. The X-ray SLD of the solution was fixed to 9.3×10^{-6} A^{-2} in all cases (average value from all fits where this parameter was free) and after that all fits were repeated. Figs. 3 and 5 present the experimental X-ray data together with the best fit results, and the parameter values from the fits are given in Table 1. The amount of incorporated AmB is calculated from surface area under curves.

3. Results and discussion

DPPC monolayers containing AmB molecules were investigated at two surface pressures: 24 mN/m and 10 mN/m. At the higher surface

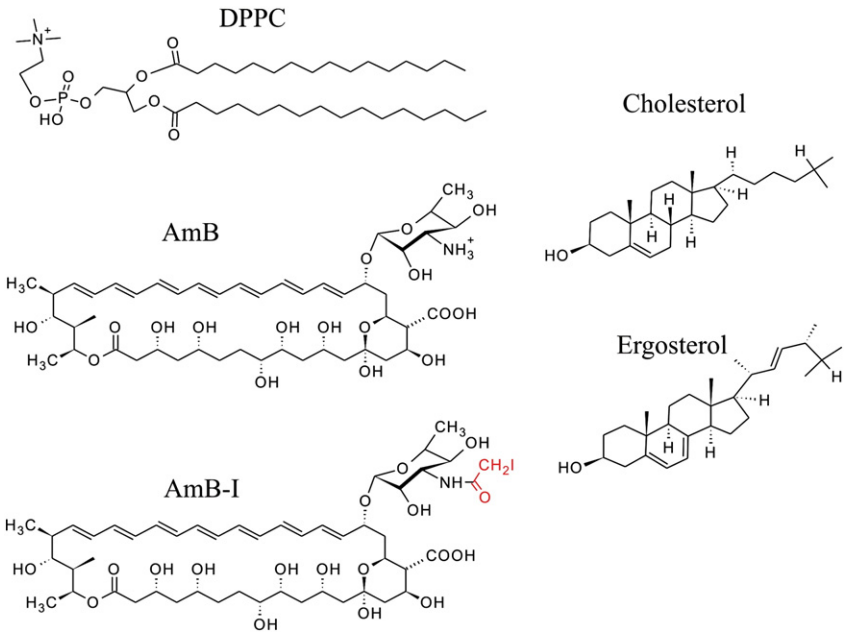

Fig. 1. Graphs of molecules used in the experiment. The N-iodoacetylamphotericin B (AmB-I) molecule is derived by substitution of the –H atom in the AmB amine group by the iodoacetate group.

Table 1
Fitting values from fits presented in Fig. 3. The layer I tail corresponds to the hydrophobic part of the lipid and the layer II head to the hydrophilic one. The error bars do not come only from statistics but also from errors at the preparation stage.

Monolayer	Thickness I layer (tails) [Å]	Thickness II layer (heads) [Å]	Total thickness [Å]	X-ray SLD I [$\times 10^{-6}$ Å^{-2}]	X-ray SLD II [$\times 10^{-6}$ Å^{-2}]	Air layer I roughness	Layer I layer II roughness	Layer II water roughness
AmB	9.4 (2)	–		18.1 (2)	–	6.6 (2)	–	2.8 (3)
Surface pressure of 10 mN/m								
DPPC	11.0 (2)	9.2 (2)	20.2 (3)	9.7 (1)	12.6 (1)	5.5 (2)	2.3 (3)	1.9 (2)
DPPC + AmB	16.7 (2)	7.1 (2)	23.8 (3)	9.83 (1)	12.5 (1)	4.3 (1)	3.3 (1)	2.4 (2)
DPPC + ergo.	14.8 (2)	7.7 (2)	22.5 (3)	10.03 (8)	11.36 (8)	4.3 (1)	2.9 (3)	1.8 (3)
DPPC + ergo. + AmB	18.9 (2)	5.2 (3)	24.1 (3)	11.0 (1)	12.98 (6)	4.6 (1)	3.0 (3)	2.8 (2)
DPPC + chole.	17.9 (2)	7.3 (1)	25.2 (2)	10.0 (1)	11.56 (6)	4.2 (1)	3.2 (2)	1.7 (2)
DPPC + chole. + AmB	17.9 (2)	8.6 (3)	25.9 (3)	11.0 (1)	12.45 (6)	4.5 (2)	3.0 (3)	2.7 (2)
Surface pressure of 24 mN/m								
DPPC	13.8 (3)	9.1 (3)	22.9 (4)	8.7 (1)	13.6 (1)	6.9 (3)	4.1 (2)	3.3 (3)
DPPC + AmB	13.9 (2)	12.5 (2)	26.4 (3)	7.6 (1)	12.6 (1)	5.3 (3)	3.6 (2)	2.2 (2)
DPPC + AmB-I	14.8 (2)	10.6 (2)	25.4 (3)	8.8 (1)	12.2 (1)	5.8 (3)	3.0 (2)	2.3 (2)

pressure, the monolayer is already tightly packed and there is not so much space for newly incoming AmB molecules from the subphase [36]. The lower surface pressure corresponds to the transition between the liquid expanded to liquid compressed phase in DPPC [37]. By choosing a surface pressure of 10 mN/m, it is easier to observe any *in situ* changes in the X-ray diffraction after AmB incorporation since more AmB molecules may be incorporated into the monolayer. Langmuir isotherms show that surface pressure changes are the most pronounced in the case of the monolayer containing ergosterol and least in the case of monolayers without sterols, see Fig. 2. This tendency is observed for both high and low surface pressures. For the higher surface pressure, the changes after AmB incorporation into the monolayer were ~5 times less pronounced than in the case of the lower surface pressure [29].

3.1. AmB incorporation into a DPPC monolayer at high surface pressure

To consider the AmB incorporation process into a DPPC monolayer, an XRR study at a surface pressure of 24 mN/m was first performed. The reference data from the pure DPPC monolayer were measured (see Fig. 3) to check their consistency with literature [38]. After AmB injection from DMSO, the system was left to stabilize for 30 min, and after that time equilibrium was reached. The XRR data are shown along with calculated X-ray SLD profiles (right panel) in Fig. 3. The comparison of DPPC monolayers containing AmB with the pure DPPC

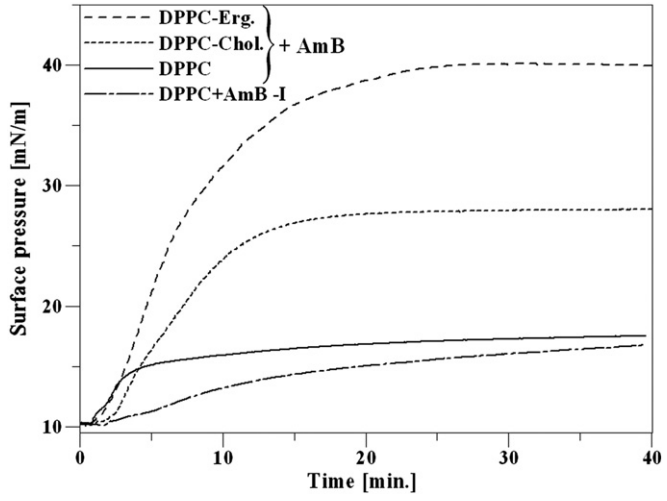

Fig. 2. Surface pressure changes after injection of AmB (2 μmol/l, pH = 12) under lipid monolayers with and without sterols at an initial surface pressure of 10 mN/m. The less pronounced surface pressure changes for AmB-I (dotted-dashed line) are caused by its higher molecular weight and better solubility in water, compared with AmB.

monolayer at this surface pressure shows that the X-ray SLD increases mostly in the hydrophobic part of the lipid monolayer. To investigate the AmB position in the monolayer more precisely, AmB-I with the same concentration in the subphase as AmB was used. The structure of this derivative is shown in Fig. 1. Although AmB-I is not as biologically active as AmB [19], it has iodine which is a good X-ray scatterer and has a significant contribution to the diffraction signal. It can be seen that after incorporation of AmB-I into the DPPC monolayer, the first oscillation at 0.2 Å^{-1} in the R/R_f curve is more pronounced, compared with those of pure DPPC and DPPC–AmB (see Fig. 3a). The oscillation amplitudes of the second maximum at 0.3 Å^{-1} in R/R_f are 0.07, 0.21, and 0.24 for DPPC, DPPC–AmB, and DPPC–AmB-I, respectively. This corresponds to a change in the X-ray SLD profiles, especially an increased SLD in layer I, *i.e.*, the tail part of the Langmuir film. AmB and AmB-I overall have a similar influence on the film structure, with some characteristic differences (see Table 1). Since AmB-I is more soluble in water than pure AmB, the distribution law predicts that a lower volume of AmB-I is incorporated into the lipid monolayer. This is confirmed by the less pronounced surface pressure changes for DPPC–AmB-I, compared with DPPC–AmB in Fig. 2 and the lower X-ray SLD for DPPC–AmB-I than for DPPC–AmB in the hydrophilic part (layer II) of the lipid monolayer (see Table 1 and Fig. 3b). It can be seen from Fig. 3b that the monolayer containing AmB-I has a higher SLD near the central part of the film around ~7 Å with respect to that of DPPC–AmB. This is also seen in the fit results giving a higher X-ray SLD of layer I for DPPC–AmB-I in comparison with DPPC–AmB (see Table 1). If the solubility of AmB-I in water were comparable to that of AmB, the content of AmB-I in the monolayer should be the same as that of AmB and thus the X-ray SLD at ~7 Å should be even higher than that observed in this experiment. The data show that the mycosamine group is located in the hydrophilic part of the DPPC monolayer both in AmB-I and AmB (see Fig. 3b). If the AmB mycosamine group were rotated with the positively charged amine group oriented towards the water surface, the shape of the X-ray SLD profile (in layer II) should be changed significantly compared with that of AmB and AmB-I, which is not the case. AmB is most probably in the dimeric form in the DPPC monolayer [3,14,16,30,39,40]; however, this cannot be verified from this experiment.

3.2. Low surface pressure

3.2.1. AmB monolayer

The pure AmB monolayer was measured 30 min after injection of the AmB solution (pH = 12) under water (final concentration 2 μmol/l in the experimental cell). In this case, the model reveals a monolayer thickness of 9.4 ± 0.2 Å, as visible in Fig. 4 (note that here and in Fig. 5 the density plot is rotated as compared with that in Fig. 3b). The corresponding reflectivity data are presented in Fig. 5a. As mentioned above, the AmB molecules in the monolayer are expected to be in aggregated forms

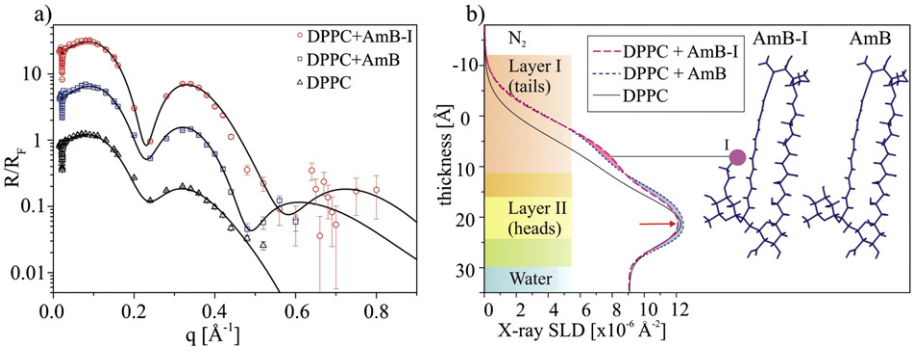

Fig. 3. a) Measured XRR data (symbols) and best fits to the model (solid lines) for the monolayers at a surface pressure of 24 mN/m. The reflectivity is normalized by the Fresnel reflectivity and plotted against the scattering vector q_z (curves for AmB are shifted by factor 5 and for AmB-I by factor 25 for better clarity. b) Interfacial X-ray SLD profiles calculated from the fits on the left and model of the derived orientation of the AmB and AmB-I molecules in the DPPC monolayer.

and lie flat on the surface, as shown in the inset of Fig. 4. These structural data on the pure AmB monolayer are a good reference point for understanding the changes observed in the lipid–sterol–AmB systems described below.

3.2.2. DPPC monolayer

Fig. 5a shows measured XRR data and best fits for monolayers at a surface pressure of 10 mN/m. Fig. 5b shows the corresponding X-ray SLD models, illustrating the effect of AmB incorporation into the DPPC monolayer at 10 mN/m. These structural changes correspond to the surface pressure changes presented in Fig. 2. It can be seen that also at the lower surface pressure the X-ray SLD of the hydrophobic part of the lipid significantly increases for AmB–DPPC (Fig. 5b, dotted-dashed line), in comparison to the pure DPPC monolayer (Fig. 5b, solid line), whereas in the hydrophilic part of the lipid the X-ray SLD decreases (see Table 1). This may suggest that part of the DPPC is involved in the complex formation between DPPC and AmB. The change of the SLD profile over the entire thickness of the film suggests that the AmB molecules in the monolayer are oriented with the longest molecular axis along the surface normal, similar as suggested for multibilayers in reference [41].

3.2.3. DPPC monolayer with ergosterol and cholesterol

In Fig. 5d, the X-ray SLD profiles of the DPPC–ergosterol and DPPC–cholesterol monolayers, both with a molar ratio of 1:1 between phospholipid and sterol, are compared. The first and main difference is the thickness of pure DPPC and DPPC–sterol mixtures. Specifically, both DPPC–ergosterol and DPPC–cholesterol monolayers are thicker by 11% and 24%, respectively, compared with the pure DPPC layer. This can be related to well-known acyl chain ordering [42] and additionally to corrugation of monolayers containing sterols. The corrugation can be

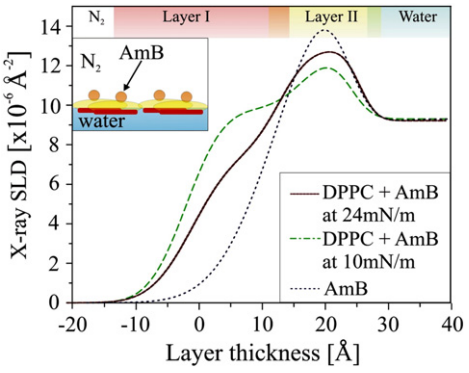

Fig. 4. Interfacial electron density profiles calculated from the fits of the pure AmB monolayer and the DPPC monolayer containing AmB at a surface pressure of 10 and 24 mN/m, showing that the changes in the X-ray SLD profile after AmB incorporation are more pronounced at the lower surface pressure. The inset shows a schematic illustration of the AmB monolayer in which the AmB molecules are oriented parallel to the surface.

caused by specific interaction between DPPC and sterols. This corrugation for cholesterol-rich membranes is significantly higher than for the ergosterol ones, which cannot be explained based purely on the acyl chain ordering. The difference between the mixtures and pure DPPC is related to the lower molecular masses of the sterols relative to DPPC in the part of the lipid polar head groups (layer II, see Fig. 5d). At the same surface pressure, this results in a lower number of scattering electrons for sterol-containing layers in this part of the X-ray SLD profile.

Not only the layer thicknesses of pure and of sterol-containing DPPC differ, but also DPPC–cholesterol layers are ~10% thicker than those of DPPC–ergosterol. One possible explanation, which however would only be relevant in the case of high sterol concentrations, is that the monolayer thickness can be affected by sterols protruding from the monolayer [43]. This is energetically unfavorable as it would require the hydrophobic part of sterol to be in contact with water. It is more probable that the ergosterol-rich monolayers are not corrugated. Moreover, X-ray SLD profiles with sterols increase mostly in the hydrophobic part of the monolayer (see Fig. 5d), which is in agreement with a previous study [43]. For these reasons, we proposed a new model in which the lipid monolayer containing cholesterol is corrugated, resulting in an increase in the (average) layer thickness (Fig. 6c). Such corrugation would explain the general increase in the thickness of DPPC containing sterols. Furthermore, a much more pronounced effect of cholesterol than of ergosterol would be expected, because of the (five times) stronger DPPC–cholesterol interaction compared with DPPC–ergosterol [8]. This hypothesis is further supported by the observed difference in surface pressure as a function of surface area [44]. As indicated in reference [44], for surface pressure of 10 mN/m, the surface areas are ~40 Å^2 and 50 Å^2 for DPPC layers containing cholesterol and ergosterol, respectively (see Fig. 6c,d). The lower value indicates that, for the same amount of molecules at the surface, the mixture of DPPC–cholesterol requires less space than that of DPPC–ergosterol. Since the sterols are similar in size, the only option to reduce the surface area for the DPPC–cholesterol system is monolayer roughness or corrugation (see Fig. 6c).

Additionally, it can be seen that the monolayer containing cholesterol has a slightly higher X-ray SLD in the hydrocarbon chain part of the lipid monolayer (−5 to 10 Å on thickness axis) as compared with the DPPC–ergosterol system while the intermediate part at 17 Å (shaded in blue in Fig. 5d) is lower. The higher X-ray SLD in the intermediate part of the lipid monolayer for ergosterol compared with cholesterol may indicate a bending of ergosterol molecules, which cannot be straight in this region because of the presence of a double bond (see Fig. 1) or lipid head group rearrangement in the presence of this sterol.

3.3. Effect of sterols on AmB incorporation

According to the XRR data (Fig. 5b,c) and in line with the surface pressure changes (Fig. 2), the presence of cholesterol or ergosterol in

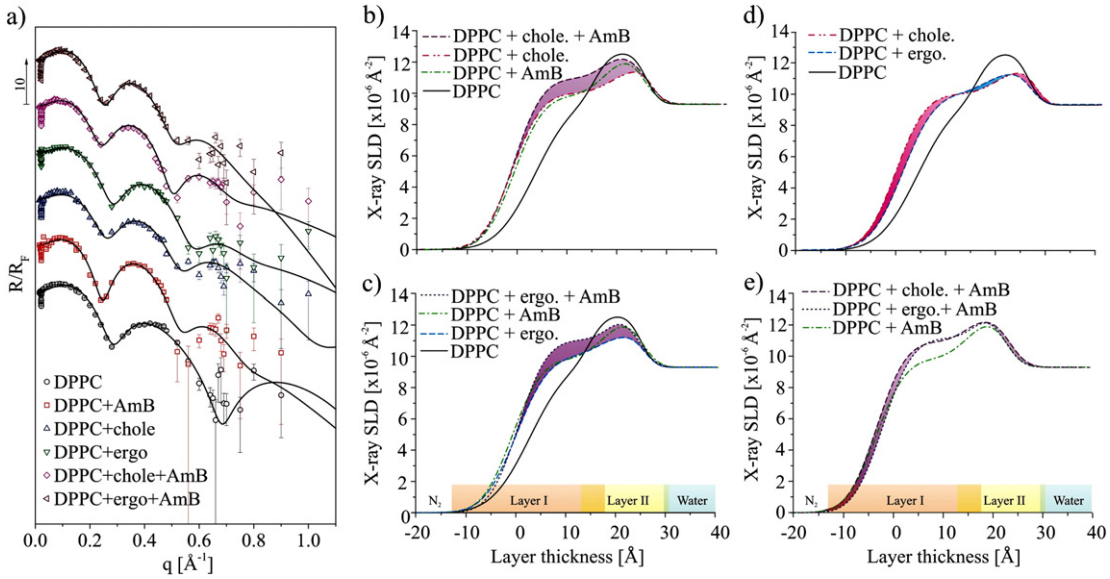

Fig. 5. (a) Measured XRR data (symbols) and best fits to model (solid lines) for monolayers at a surface pressure of 10 mN/m. For clarity, the data have been offset vertically. (b–d) Interfacial X-ray SLD profiles calculated from the fits in panel a (see text for details).

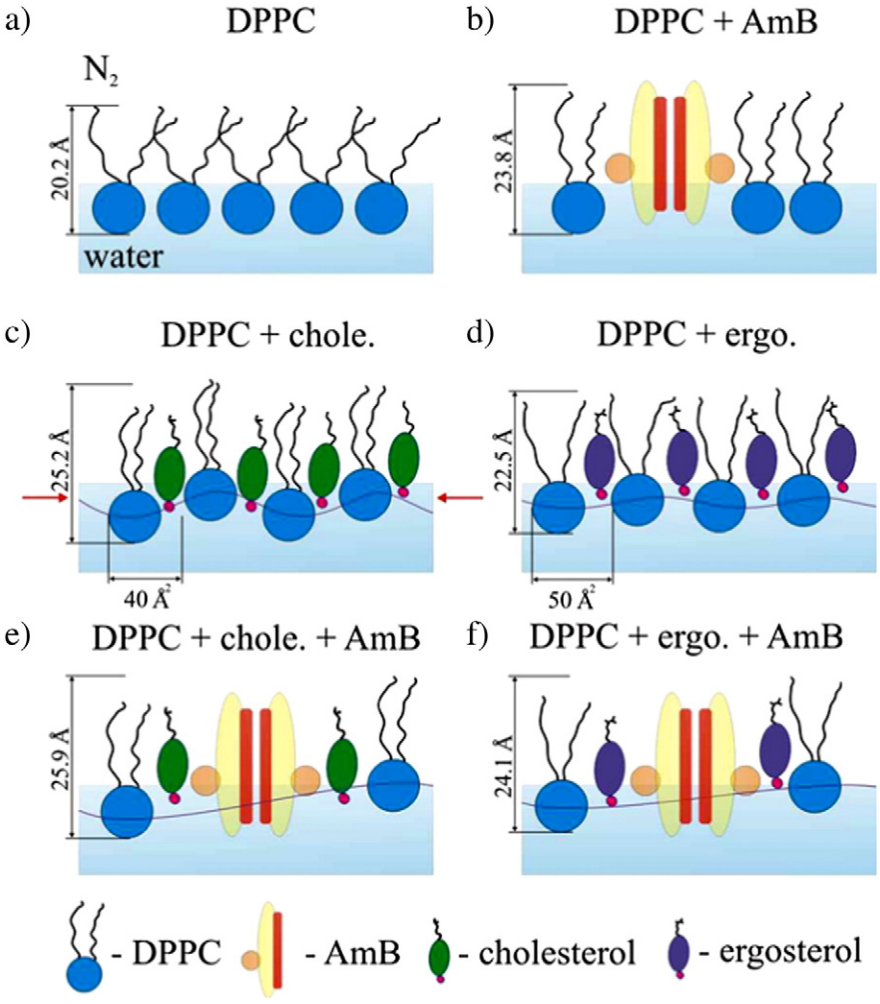

Fig. 6. Schematic models of the lipid layer structure derived from the X-ray SLD profiles. The red strip in the AmB molecules represents the polyol subunit, which is rich in –OH groups. Arrows on panel c indicate the surface compression caused by monolayer corrugation/buckling, leading to smaller molecular surface area.

the Langmuir film results in a significantly larger incorporation of AmB than for the DPPC monolayer without sterols. This can be explained by the spacer effect of sterols which facilitate AmB incorporation into the lipid monolayer. The measured layer thickness varies in all studied systems, as can be seen in Fig. 5 and Table 1, with the thinnest layers belonging to DPPC (20.2 Å) and the thickest layers belonging to DPPC–cholesterol–AmB (25.9 Å). Fig. 5c shows a comparison between Langmuir films of pure DPPC, DPPC containing ergosterol (layer thickness 22.5 Å), and a mix of DPPC with ergosterol and AmB (layer thickness 24.1 Å). Fig. 5b presents the corresponding data for pure DPPC, DPPC containing cholesterol (layer thickness 25.2 Å), and a mix of DPPC with cholesterol and AmB (layer thickness 25.9 Å). It can be seen that in both cases the amount of incorporated AmB into the monolayer is similar, *i.e.*, there is a ~20% increase in X-ray SLD compared to AmB in the pure DPPC (see Fig. 5e).

This is contrary to the interpretation based purely on the surface pressure changes where a higher surface pressure is generally interpreted as an indication of a greater amount of AmB incorporation into the monolayer [36]. The XRR observations suggest that the more pronounced surface pressure changes in the presence of ergosterol (see Fig. 2) are caused by changes in the film structure rather than in the amount of incorporated molecules. Specifically, the data clearly show that, similar to the DPPC–sterol monolayers, the DPPC–cholesterol–AmB monolayer is also 10% thicker than the DPPC–ergosterol–AmB monolayer (tails + heads). Together with the roughness increase from 1.7 to 2.7, this suggests that the layer of DPPC–cholesterol–AmB is rough or corrugated/buckled, whereas the DPPC–ergosterol–AmB remains smoother. The increased thickness of DPPC–ergosterol–AmB as compared with DPPC–ergosterol layers is most likely caused by the vertical extension of the AmB, since it is within the experimental errors identical to the thickness of DPPC–AmB. A more detailed analysis of Fig. 5e reveals that the X-ray SLD profiles of monolayers containing sterols and AmB increase similarly in Layer I and Layer II (see Fig. 5e). This suggests that AmB molecules are standing up, with the longest axis perpendicular to the surface (see Fig. 6e,f).

4. Conclusions

In summary, we present for the first time structural data for AmB incorporation into DPPC monolayers at surface pressures of 10 mN/m and 24 mN/m, which provides insight into the location and orientation of AmB molecules in the lipid layer. It is clear from the experimental results that the mycosamine group of iodine-marked AmB (AmB-I) is located in the hydrophilic (Layer II) part of the lipid monolayer and that AmB-I are oriented with the long axis perpendicular to the surface. Because the X-ray SLD profiles for AmB are very similar to the one of AmB-I, it can be concluded that both molecules and mycosamine subunits have a similar orientation in the monolayer.

The most important result concerns differences between the X-ray SLD profiles of DPPC–cholesterol and DPPC–ergosterol monolayers. In the case of cholesterol, the monolayer is thicker, suggesting monolayer corrugation/buckling due to stronger interactions between the sterol and DPPC. Surprisingly, the difference between DPPC–cholesterol and DPPC–ergosterol does not influence the amount of AmB incorporation into the monolayer. In both cases, the density of AmB incorporated in the monolayer is the same according to the XRR data, indicating that the monolayer availability for AmB is the same for these two sterols. This observation is apparently contrary to the surface pressure changes where the biggest differences are observed for DPPC–ergosterol–AmB, while the one for DPPC–cholesterol–AmB are almost two-fold smaller. However, this discrepancy can be explained by structural differences of ergosterol- and cholesterol-containing DPPC layers. Similar to the DPPC–cholesterol, also the DPPC–cholesterol–AmB monolayers have a larger average thickness than their ergosterol-containing counterparts. Taking into account these X-ray results and surface pressure changes, it can be concluded that the DPPC–cholesterol–AmB monolayer is also corrugated/buckled while the DPPC–ergosterol–AmB monolayer is more flat. To test the buckling hypothesis we design a new experiment with marked lipid molecules.

The buckling effect can influence the aggregation process of AmB in membranes and thus formation of pores. For more flat ergosterol-rich membranes this can lead to the formation of well shaped pores while for cholesterol-rich membranes the buckling can be responsible for the formation of aggregates.

Acknowledgements

This research was financed by the National Science Centre of Poland on the basis of decision no. DEC-2012/05/B/NZ1/00037. The X-ray measurements were financed by PETRA III in DESY (Germany). LISA is supported by the Bundesministerium für Bildung und Forschung (BMBF) (Project 05KS10FK2). We would like to thank the PETRA III staff for kind assistance during the experiment.

References

[1] H.A. Gallis, R.H. Drew, W.W. Pickard, Amphotericin B: 30 years of clinical experience, Rev. Infect. Dis. 12 (1990) 308–329.
[2] S. Hartsel, J. Bolard, Amphotericin B: new life for an old drug, Trends Pharmacol. Sci. 17 (1996) 445–449.
[3] K.C. Gray, D.S. Palacios, I. Dailey, M.M. Endo, B.E. Uno, B.C. Wilcock, M.D. Burke, Amphotericin primarily kills yeast by simply binding ergosterol, Proc. Natl. Acad. Sci. 109 (2012) 2234–2239.
[4] M. Gagoś, J. Gabrielska, M. Dalla Serra, W.I. Gruszecki, Binding of antibiotic amphotericin B to lipid membranes: monomolecular layer technique and linear dichroism-FTIR studies, Mol. Membr. Biol. 22 (2005) 433–442.
[5] S.C. Kinsky, S.A. Luse, L.L.N.V. Deenen, Fed. Proc. Fed. Am. Soc. Exp. Biol. (1996) 1503.
[6] B.C. Wilcock, M.M. Endo, B.E. Uno, M.D. Burke, C2′-OH of amphotericin B plays an important role in binding the primary sterol of human cells but not yeast cells, J. Am. Chem. Soc. 135 (2013) 8488–8491.
[7] W.I. Gruszecki, M. Gagoś, M. Herec, P. Kernen, Organization of antibiotic amphotericin B in model lipid membranes. A mini review, Cell. Mol. Biol. Lett. 8 (2003) 161–170.
[8] K. Hac-Wydro, P. Dynarowicz-Latka, J. Grzybowska, E. Borowski, Interactions of Amphotericin B derivative of low toxicity with biological membrane components — the Langmuir monolayer approach, Biophys. Chem. 116 (2005) 77–88.
[9] N. Matsumori, Y. Sawada, M. Murata, Mycosamine orientation of amphotericin B controlling interaction with ergosterol: sterol-dependent activity of conformation-restricted derivatives with an amino-carbonyl bridge, J. Am. Chem. Soc. 127 (2005) 10667–10675.
[10] N. Matsumori, Y. Sawada, M. Murata, Large molecular assembly of amphotericin B formed in ergosterol-containing membrane evidenced by solid-state NMR of intramolecular bridged derivative, J. Am. Chem. Soc. 128 (2006) 11977–11984.
[11] J. Miñones Jr., O. Conde, P. Dynarowicz-Łątka, M. Casas, Penetration of amphotericin B into DOPC monolayers containing sterols of cellular membranes, Colloids Surf. A Physicochem. Eng. Asp. 270–271 (2005) 129–137.
[12] A. Neumann, M. Baginski, J. Czub, How do sterols determine the antifungal activity of amphotericin B? Free energy of binding between the drug and its membrane targets, J. Am. Chem. Soc. 132 (2010) 18266–18272.
[13] A. Neumann, M. Baginski, J. Czub, Exploring amphotericin B-membrane interactions: free energy simulations, Biophys. J. 104 (2013) 250a–250a.
[14] Y. Umegawa, Y. Nakagawa, K. Tahara, H. Tsuchikawa, N. Matsumori, T. Oishi, M. Murata, Head-to-tail interaction between amphotericin B and ergosterol occurs in hydrated phospholipid membrane, Biochemistry 51 (2012) 83–89.
[15] T.M. Anderson, M.C. Clay, A.G. Cioffi, K.A. Diaz, G.S. Hisao, M.D. Tuttle, A.J. Nieuwkoop, G. Comellas, N. Maryum, S. Wang, B.E. Uno, E.L. Wildeman, T. Gonen, C.M. Rienstra, M.D. Burke, Amphotericin forms an extramembranous and fungicidal sterol sponge, Nat. Chem. Biol. 10 (2014) 400-U121.
[16] P. Dynarowicz-Latka, J. Minones, O. Conde, M. Casas, E. Iribarnegaray, BAM studies on the penetration of amphotericin B into lipid mixed monolayers of cellular membranes, Appl. Surf. Sci. 246 (2005) 334–341.
[17] P. Dynarowicz-Latka, R. Seoane, J. Minones, M. Velo, J. Minones, Study of penetration of amphotericin B into cholesterol or ergosterol containing dipalmitoyl phosphatidylcholine Langmuir monolayers, Colloids Surf. B 27 (2003) 249–263.
[18] K. Hac-Wydro, P. Dynarowicz-Latka, Interaction between nystatin and natural membrane lipids in Langmuir monolayers—the role of a phospholipid in the mechanism of polyenes mode of action, Biophys. Chem. 123 (2006) 154–161.
[19] K. Hac-Wydro, P. Dynarowicz-Latka, J. Grzybowska, E. Borowski, How does the N-acylation and esterification of amphotericin B molecule affect its interactions with cellular membrane components—the Langmuir monolayer study, Colloids Surf. B: Biointerfaces 46 (2005) 7–19.
[20] M. Gagoś, M. Arczewska, FTIR spectroscopic study of molecular organization of the antibiotic amphotericin B in aqueous solution and in DPPC lipid monolayers containing the sterols cholesterol and ergosterol, Eur. Biophys. J. 41 (2012) 663–673.

[21] J. Barwicz, P. Tancrede, The effect of aggregation state of amphotericin-B on its interactions with cholesterol- or ergosterol-containing phosphatidylcholine monolayers, Chem. Phys. Lipids 85 (1997) 145–155.
[22] P. Wydro, S. Knapczyk, M. Lapczynska, Variations in the condensing effect of cholesterol on saturated versus unsaturated phosphatidylcholines at low and high sterol concentration, Langmuir 27 (2011) 5433–5444.
[23] H.M. McConnell, A. Radhakrishnan, Condensed complexes of cholesterol and phospholipids, BBA Biomembr. 1610 (2003) 159–173.
[24] P. Somerharju, J.A. Virtanen, K.H. Cheng, M. Hermansson, The superlattice model of lateral organization of membranes and its implications on membrane lipid homeostasis, BBA Biomembr. 1788 (2009) 12–23.
[25] D. Kaminski, P. Poodt, E. Aret, N. Radenovic, E. Vlieg, Surface alloys, overlayer and incommensurate structures of Bi on Cu(111), Surf. Sci. 575 (2005) 233–246.
[26] J.J. Pan, T.T. Mills, S. Tristram-Nagle, J.F. Nagle, Cholesterol perturbs lipid bilayers nonuniversally, Phys. Rev. Lett. 100 (2008).
[27] J.J. Pan, S. Tristram-Nagle, J.F. Nagle, Effect of cholesterol on structural and mechanical properties of membranes depends on lipid chain saturation, Phys. Rev. E. 80 (2009).
[28] K.N. Jarzembska, D. Kaminski, A.A. Hoser, M. Malinska, B. Senczyna, K. Wozniak, M. Gagoś, Controlled crystallization, structure, and molecular properties of iodoacetylamphotericin B, Cryst. Growth Des. 12 (2012) 2336–2345.
[29] M.J. Paquet, I. Fournier, J. Barwicz, P. Tancrede, M. Auger, The effects of amphotericin B on pure and ergosterol- or cholesterol-containing dipalmitoylphosphatidylcholine bilayers as viewed by H-2 NMR, Chem Phis. Lipids 119 (2002) 1–11.
[30] M. Gagoś, M. Herec, M. Arczewska, G. Czernel, M. Dalla Serra, W.I. Gruszecki, Anomalously high aggregation level of the polyene antibiotic amphotericin B in acidic medium: implications for the biological action, Biophys. Chem. 136 (2008) 44–49.
[31] B.M. Murphy, M. Greve, B. Runge, C.T. Koops, A. Elsen, J. Stettner, O.H. Seeck, O.M. Magnussen, A new diffractometer for studies of liquid–liquid interfaces, Am. Inst. Phys. Conf. Proc. 1234 (2010) 155–158.
[32] B.M. Murphy, M. Greve, B. Runge, C.T. Koops, A. Elsen, J. Stettner, O.H. Seeck, O.M. Magnussen, A novel X-ray diffractometer for studies of liquid–liquid interfaces, J. Synchrotron Radiat. 21 (2014) 45–56.
[33] O.H. Seeck, C. Deiter, K. Pflaum, F. Bertam, A. Beerlink, H. Franz, J. Horbach, H. Schulte-Schrepping, B.M. Murphy, M. Greve, O. Magnussen, The high-resolution diffraction beamline P08 at PETRA III, J. Synchrotron Radiat. 19 (2012) 30–38.
[34] A. Nelson, Co-refinement of multiple-contrast neutron/X-ray reflectivity data using MOTOFIT, J. Appl. Crystallogr. 39 (2006) 273–276.
[35] O. Heavens, Optical Properties of Thin Solid Films, Butterworth Scientific Publications, London, 1955.
[36] P. Dynarowicz-Łątka, R. Seoane, J. Miñones Jr., M. Velo, J. Miñones, Study of penetration of amphotericin B into cholesterol or ergosterol containing dipalmitoyl phosphatidylcholine Langmuir monolayers, Colloids Surf. B: Biointerfaces 27 (2003) 249–263.
[37] G. Ma, H.C. Allen, DPPC Langmuir monolayer at the air–water interface: probing the tail and head groups by vibrational sum frequency generation spectroscopy, Langmuir 22 (2006) 5341–5349.
[38] G. Wu, J. Majewski, C. Ege, K. Kjaer, M.J. Weygand, K.Y. Lee, Interaction between lipid monolayers and poloxamer 188: an X-ray reflectivity and diffraction study, Biophys. J. 89 (2005) 3159–3173.
[39] M. Gagoś, W.I. Gruszecki, Organization of polyene antibiotic amphotericin B at the argon–water interface, Biophys. Chem. 137 (2008) 110–115.
[40] M. Gagoś, R. Koper, W.I. Gruszecki, Spectrophotometric analysis of organisation of dipalmitoylphosphatidylcholine bilayers containing the polyene antibiotic amphotericin B, Biochim. Biophys. Acta 1511 (2001) 90–98.
[41] F. Foglia, M.J. Lawrence, B. Deme, G. Fragneto, D. Barlow, Neutron diffraction studies of the interaction between amphotericin B and lipid–sterol model membranes, Sci. Rep. 2 (2012).
[42] J. Czub, M. Baginski, Comparative molecular dynamics study of lipid membranes containing cholesterol and ergosterol, Biophys. J. 90 (2006) 2368–2382.
[43] A. Ivankin, I. Kuzmenko, D. Gidalevitz, Cholesterol–phospholipid interactions: new insights from surface X-ray scattering data, Phys. Rev. Lett. 104 (2010) 108101.
[44] K. Sabatini, J.P. Mattila, P.K.J. Kinnunen, Interfacial behavior of cholesterol, ergosterol, and lanosterol in mixtures with DPPC and DMPC, Biophys. J. 95 (2008) 2340–2355.